Implementation and test of spatially varying (climatological and flow-dependent) background error variances in Aladin

Benedikt Strajnar
University of Ljubljana
benedikt.strajnar@rzs-hm.si

Météo France stay report
Supervisor: Loïk Berre
Toulouse, 7^{th} January - 14^{th} February 2008

June 4, 2008

Contents

1. Introduction

Inside variational data assimilation, one has to provide the background error statistics for computing the background part of variational cost function. They can be estimated using different error simulation approaches. For the work presented in this report, the short-range forecasts provided by an Arpege assimilation ensemble (Berre et al 2007) are used. The statistics contain cross- and auto-covariances, which determine the spatial amplitude and structure of analysis increments (described to detail in Berre (2000)). At first order, the amplitude of increments is basically determined by standard deviations of background error (σ_b, hereafter often called simply background errors).

In Arpege/IFS/Aladin, the minimization procedure is performed in spectral space rather than grid point (physical) space. Conceptually, the vector of increments is projected in a way to obtain a control variable with the covariance matrix equal identity. This simplifies the cost function and improves convergence of the minimization. One of the steps in this variable change is the normalization by background error standard deviations. If this is done in spectral space, the horizontally-averaged values are used (over all spectral coefficients m, n). The errors have therefore no geographical dependence. This might be an oversimplification, since it is well known that background errors are not uniform over the globe, but are higher in data-poor regions and when the weather situation is dynamically active. The other option is to perform normalization in grid point space, which requires an additional forward and backward spectral transform. This is already present for Arpege global model. Moreover, horizontally-averaged σ_b's are usually climatological (i.e. averaged in time over several weeks). In contrast, grid point σ_b's will be here specified either climatologically, or in a flow-dependent way.

The aim of my stay was to adapt normalization in grid point space to Aladin, using horizontally and vertically varying relative vorticity background errors, estimated from an ensemble of Arpege analyses and short range forecasts (see Belo Pereira and Berre (2006) and Berre et al 2007). The variance maps were normalized in such a way that their horizontal average matched the Aladin spectral average. For other variables, spectral average background errors were still used. The exception was specific humidity background errors, which were made flow-dependent by using an empirical formula (Rabier et al. (1998)), depending on background temperature and relative humidity. The required technical steps to prepare grid point errors for limited area model are described to more details in the technical documentation (see appendix).

The comparisons inside Aladin FRANCE 3DVAR were first carried out between climatological (constant) background error values and the reference spectral normalization. Finally, the daily "flow dependent" values of background errors were used, and compared to the operational reference. Some case studies were considered around an interesting period of cold air cutoff within the comparison period.

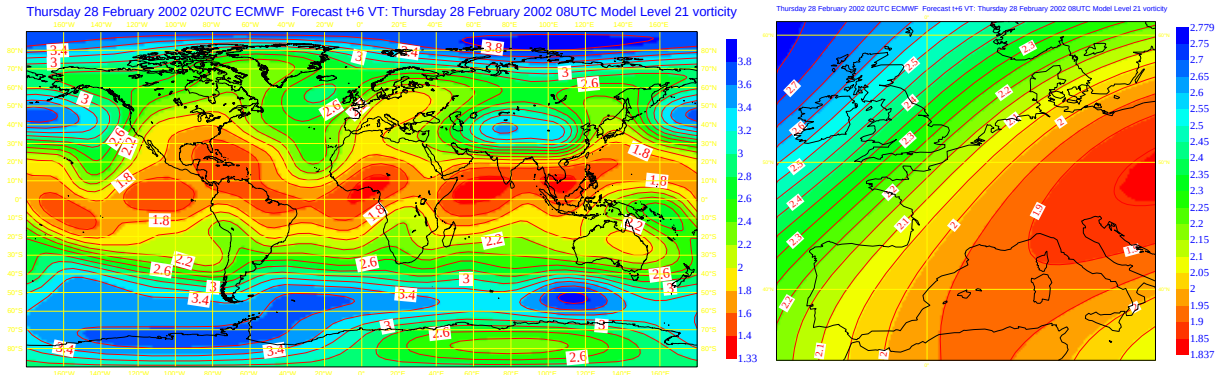

Figure 1: Climatological ensemble σ_b maps for relative vorticity at level 21 (approximately 500 hPa): global (left) and zoom over Europe (right). Unit is 10^{-5}/s.

2. Climatological horizontal background errors

2.1. Maps of background errors

Specification of climatological background errors allow us to account for the fact that the accuracy of background is not constant over the globe, even in a time-averaged sense. This arises mainly from the different quality of initial conditions over the areas of different data density, but can also rely on the atmospheric flow properties (errors higher over areas of frequent cyclogenesis, jet stream positions etc.). Experiments were first carried out using climatological background errors, obtained by a six member Arpege ensemble in a period of February and March 2002. The horizontal maps of background errors are specified for each of 41 vertical levels. In the middle troposphere (figure 1), the errors are larger over polar regions (especially in the south hemisphere) and over the oceans. Errors are smaller over tropical regions and, as a result of good observational data coverage, also over the most populated parts of the continents. Opposite situation can be found in the stratosphere, where the values are higher over tropics. The ratio of small and high background errors in the mid-troposphere is around 2 on the globe, and around 1.4 over the domain of Aladin France.

This approach seems to be more realistic compared to using average spectral errors. With such an error specification, we expect to decrease the analysis fit to observations over data-dense regions (continental Europe in our case), and increase it over the Atlantic Ocean and north-western part of Europe.

2.2. Diagnostic full observation experiments

After applying the changes to the code, first experiments were performed for the purpose of diagnostics. The very first goal was to test if the σ_b map is correctly read, interpolated to Aladin geometry, rescaled and applied in the minimization procedure. To do this, the differences, against a reference analysis using average background errors in spectral space, have been plotted. Expected behavior of analysis increments is shown in figure 2, where the increments slightly differ only over Northern UK and near Denmark for instance. Because

of higher σ_b values in this region (see figure 1), the 400 hPa analysis increments are larger (i.e. the analysis is closer to observations).

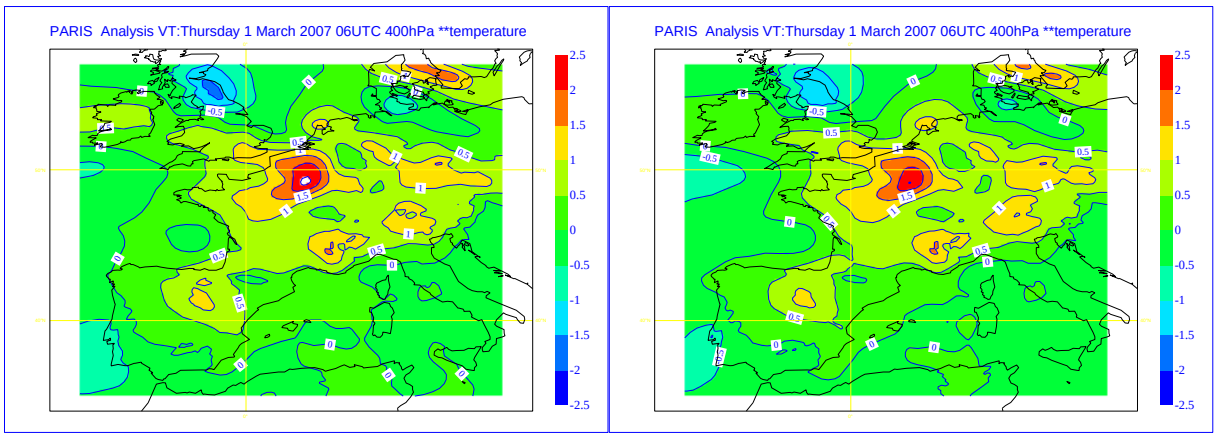

Figure 2: 400 hPa temperature analysis increments on March 3^{th} 2007 6 UTC using climatological background errors (left) and average spectral errors (right).

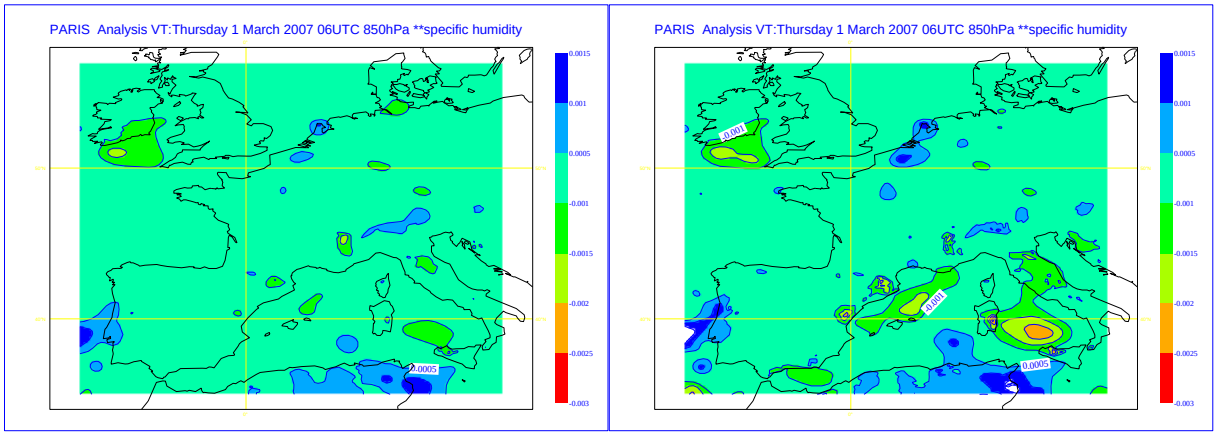

Figure 3: 850 hPa specific humidity (kg/kg) analysis increments on March 3^{th} 2007 6 UTC using Undén's flow-dependent formula (left) and average spectral errors (right).

Another even more significant difference is found for specific humidity increments (figure 3, see area north to Sicily). The humidity background error is now horizontally varying and depends on background values of relative humidity and temperature (Rabier et al. (1998)). Relative humidity background error is calculated as

$$\sigma_b = -0.002T_b - 0.003(T_b - 273) + 0.35(RH_b - 0.4) + 0.70$$

$$0.06 < \sigma_b < 0.18$$

and then converted to specific humidity background error by a simple relation (inverting the relative humidity formula basically) and adjusted near the surface. In our further experiments, the identified impact is always a sum of vorticity and humidity background error changes, which were not studied independently.

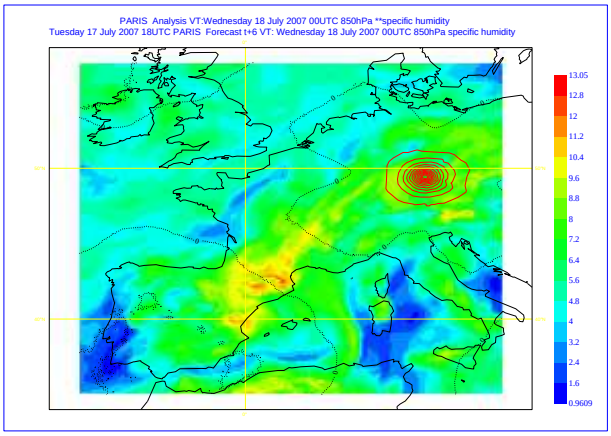

Figure 4: Analysis increment of specific humidity (isoline density 0.0001 kg/kg) on July 18^{th} 2007 0 UTC using single observation at 850 hPa climatological (vorticity) and flow-dependent (humidity) background errors.

2.3. Single observation experiments

Single observation experiments are an attractive diagnostic tool, because we can compare the actual analysis increments values to theoretical ones. The value of analysis increment is exactly known and equals

$$\delta x_a = \frac{\sigma_b^2}{\sigma_o^2 + \sigma_b^2}(y - Hx_b),$$

where σ_o is standard deviation of observational error and $y - Hx_b$ is the departure of observation y from the background Hx_b. Using the standard definition of observational cost function $J_o = \frac{(y-Hx)^2}{2\sigma_o^2}$, we get the expression for effective σ_b, that was used in minimization:

$$\sigma_b = \sigma_o \sqrt{\sqrt{\frac{J_o^{start}}{J_o^{end}}} - 1}.$$

J_o^{start} is the value of cost function at the beginning of minimization and J_o^{end} is the cost function after convergence is achieved. This is a way to verify that the used background errors really correspond to the prescribed values. By comparing two single observations at different geographical locations, one can observe the effects of the horizontal dependence of background error σ_b. Such comparisons were especially useful to estimate the humidity background errors, since their map is not directly available. The strong dependence of σ_b to background humidity can be verified by comparing amplitudes of figures 3 and 4. If humidity (and possibly temperature) is high, the observation increments are allowed to be higher.

2.4. Long term impact runs

After a validation of grid point $\sigma_b's$, two long term impact runs were designed. The first one (called WINTER), was performed for the period of January 7^{th} 2007 - February 2^{th} 2007 and the second one (called SUMMER) for the period between July 18^{th} 2007 and August 16^{th} 2007. Periods in different seasons of the year were chosen in order to evaluate the performance

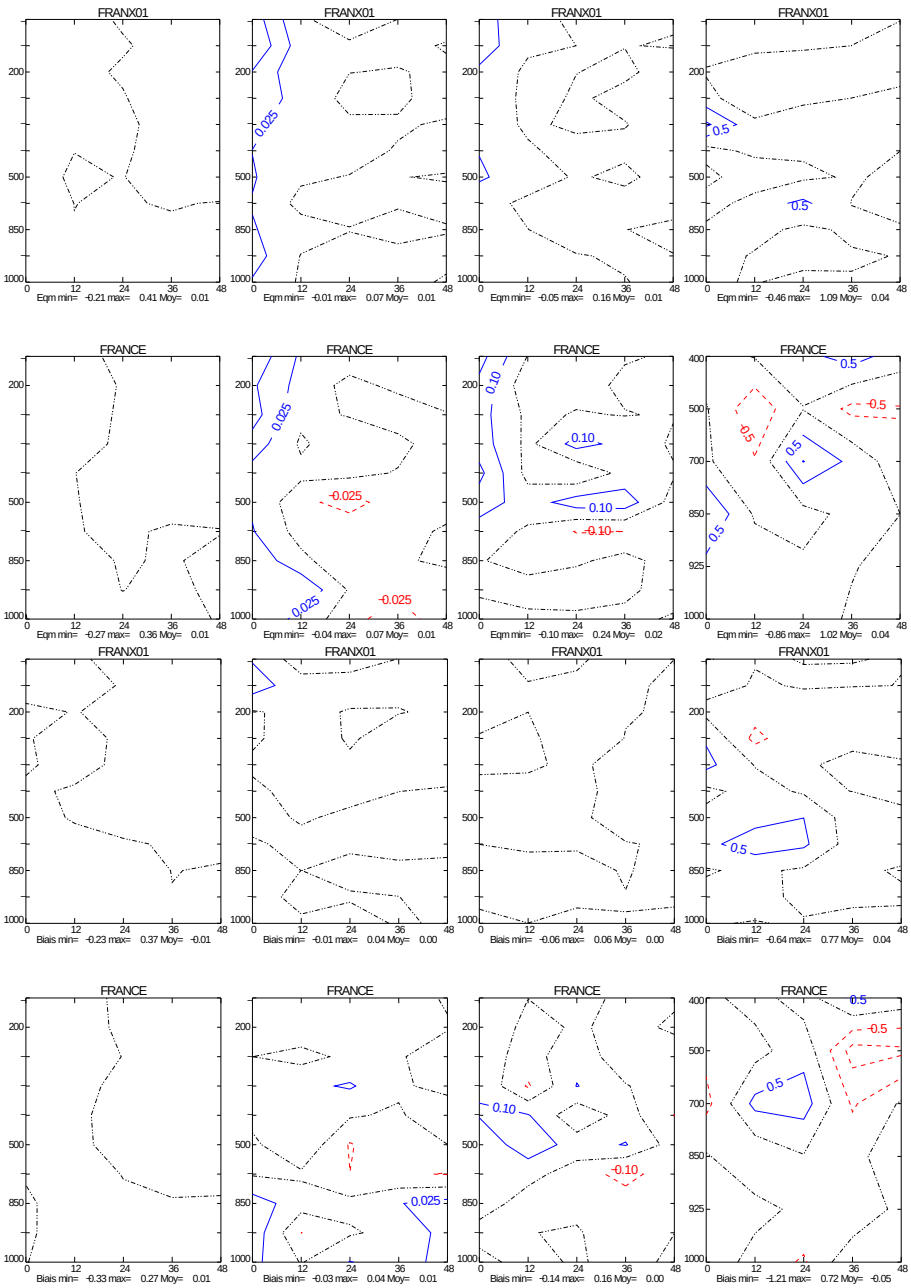

Figure 5: RMSE (top) and bias (bottom) cross sections computed against TEMP on two different domains (WINTER period). From left to right: geopotential (0.5 m contours), temperature (0.025 K), wind (0.1 m/s) and relative humidity (0.5 %).

of grid point climatological vorticity errors and flow-dependent specific humidity errors in different conditions. The assimilation cycle frequency was 6 hours and production run of 48 hours was performed once a day at 0 UTC. As a reference, the experiments corresponding to operational 3DVAR (using average spectral background errors) were used. The scores were computed against radiosoundings (TEMP) over the FRANX01 domain, which covers the majority of computational domain, and separately over France. Figures 5 and 7 present the root mean square and bias scores (reference minus experiment) at different vertical

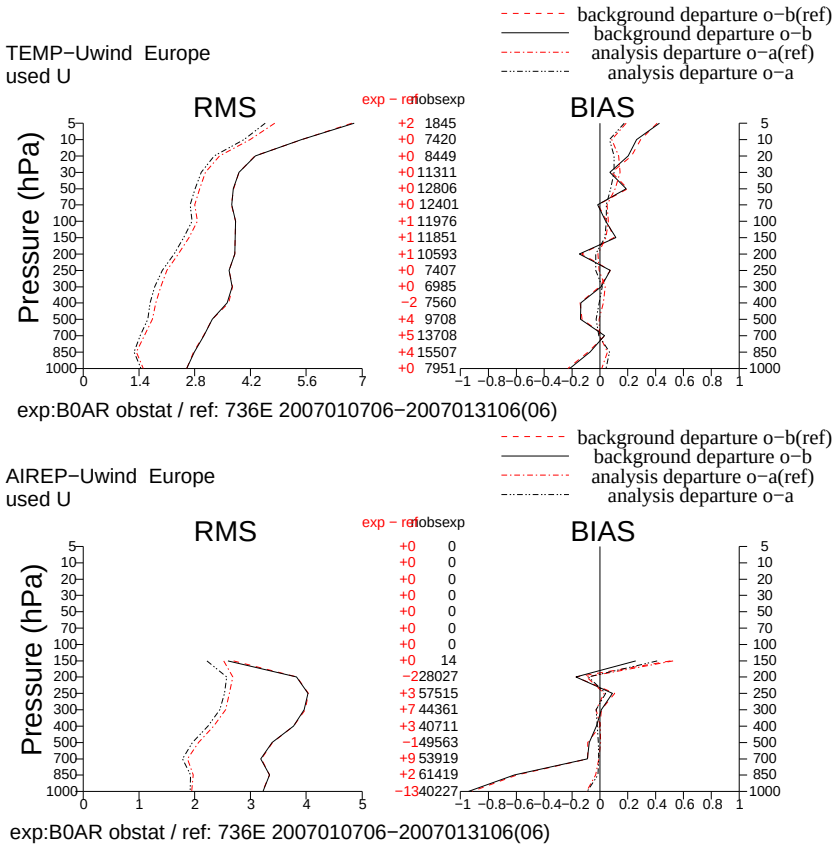

Figure 6: Observational statistics for TEMP (left) and AIREP (right) observations in WINTER period.

levels and forecast ranges. The positive values (in blue) correspond to improved scores and negative (in red) to degradations. To first concentrate on the WINTER period, we can notice that the temperature and wind RMS at analysis time are smaller using grid point background errors. That means that analysis fits more to the observations. This is itself no indication of improvement, but for low-level temperature over France, small improvements can be detected also at 12-hour forecast range. Verification over France indicates a slightly positive impact on wind RMSE and relative humidity forecast bias. The effect in the analysis was investigated also by checking the analysis departures from observations and background (*obstat* program). The results show an increased fit at all levels for most of observation types (TEMP and AIREP in figure 6 as an example), but this generally does not cause improved fit of first guesses.

In the SUMMER period, there is no pronounced difference at analysis time. Over FRANX01 domain, a degradation is observed for relative humidity in the upper troposphere at 12h range (bias and RMSE). For wind, a relatively large improvement is observed at 12h range near the jet level over France.

To conclude the experiments, the impact is nearly neutral globally and slightly positive for wind, and also for humidity in winter. This means that such climatological errors, although computed for a relatively short time period (a few weeks), can be successfully used

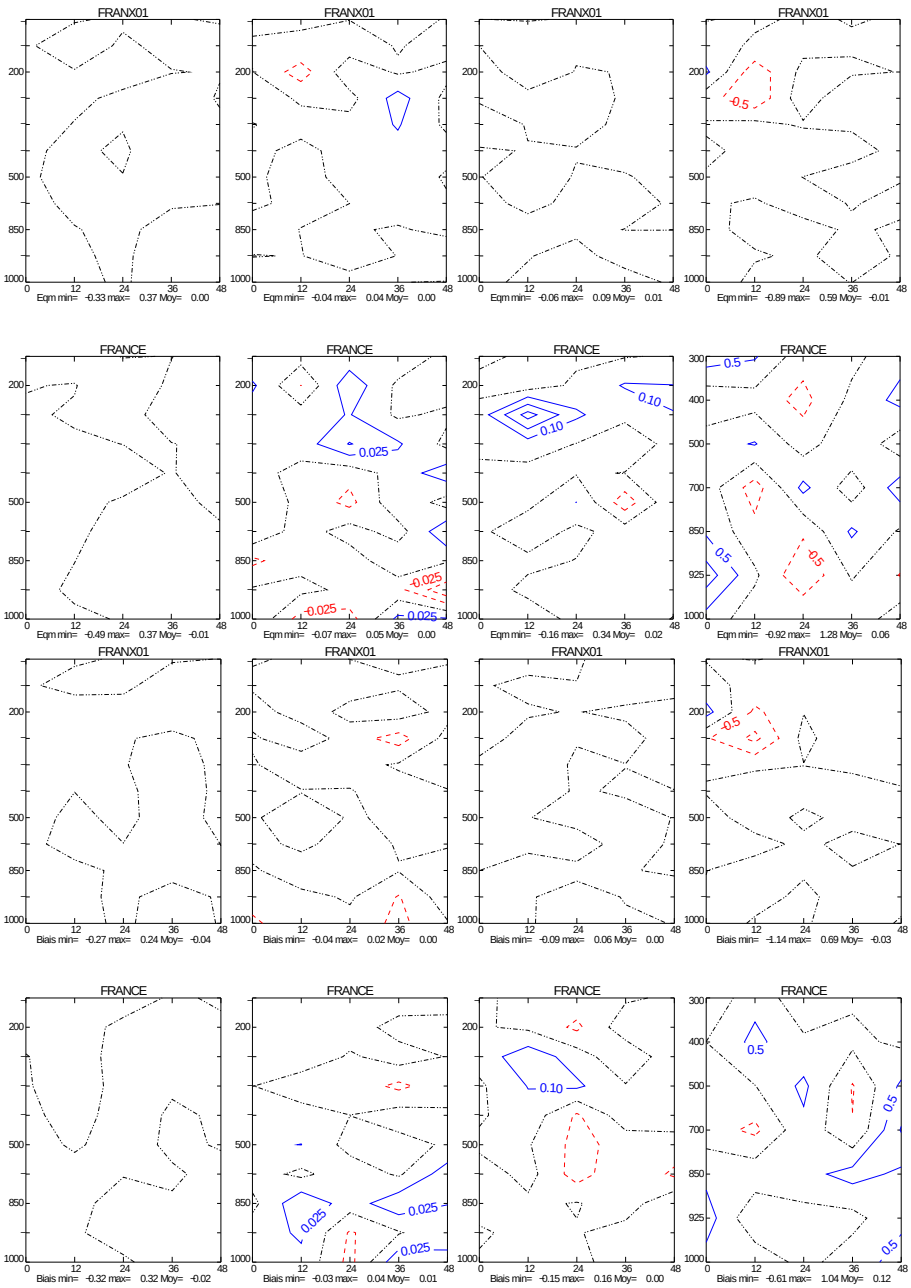

Figure 7: RMSE (top) and bias (bottom) cross sections computed against TEMP on two different domains (SUMMER period). From left to right: geopotential (0.5 m contours), temperature (0.025 K), wind (0.1 m/s) and relative humidity (0.5 %).

inside minimization. The sensitivity of climatological background errors to the time period for averaging has however not been investigated yet.

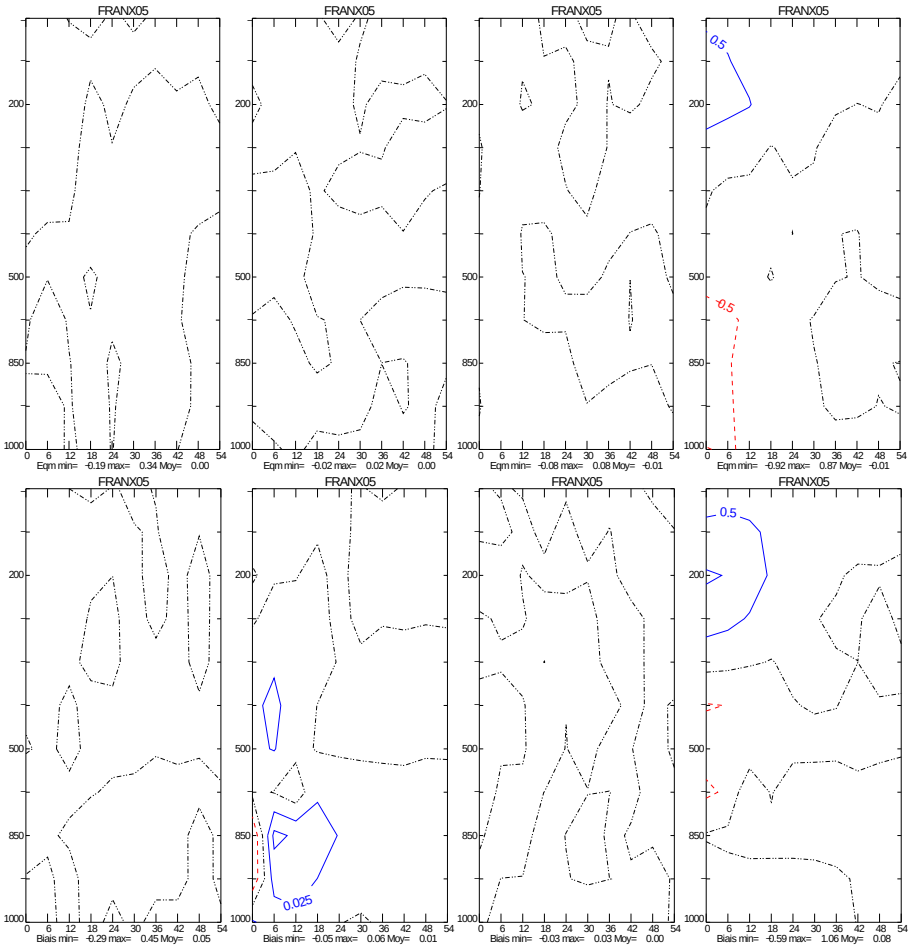

Figure 8: RMSE (top) and bias (bottom) cross sections computed against ECMWF analysis (SBDAY period). From left to right: geopotential (0.5 m contours), temperature (0.025 K), wind (0.1 m/s) and relative humidity (0.5 %).

3. Errors of the day

3.1. Long term impact runs

After investigating the impacts of climatological values, the natural continuation is to test the background errors of the day. This means that geographical maps of background error for different vertical levels are computed for each analysis using Arpege ensemble. As mentioned before, the normalization with average spectral values is performed in order to represent the finer resolution of grid of Aladin. The long-term impact run (called SBDAY) was performed for a period of 8^{th} September - 5^{th} October 2007. For this period, a six-member Arpege ensemble was available to simulate background errors. Forecast errors were specified at 60 vertical levels, with horizontal resolution of 1.5 degree. The comparison against operational Aladin France was done, using TEMP observations and ECMWF analysis for the reference.

Besides computing time-averaged difference of scores, another interesting possibility is to plot also the daily evolution of scores for different variables and vertical levels. The scores generally do not change dramatically, but one can identify some predominant improvements

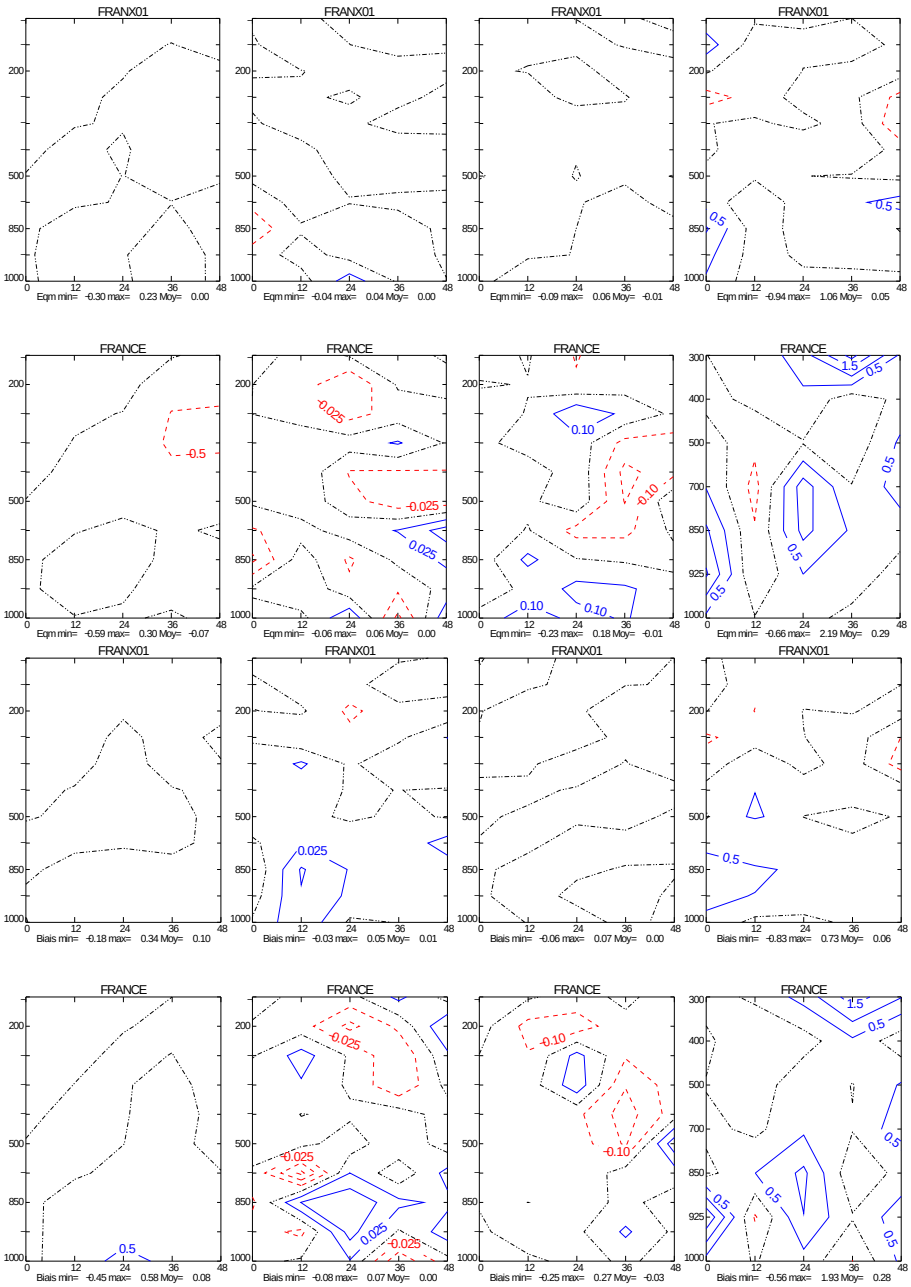

Figure 9: RMSE (top) and bias (bottom) cross sections computed against TEMP on two different domains (SBDAY period). From left to right: geopotential (0.5 m contours), temperature (0.025 K), wind (0.1 m/s) and relative humidity (0.5 %).

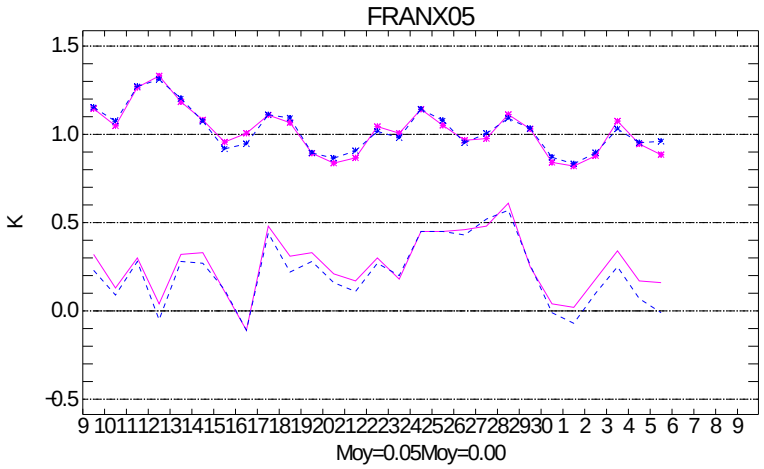

Figure 10: Daily evolution of forecast RMSE and bias for 850 hPa +12h temperature forecast against ECMWF analysis. Experiment is in blue color and the reference in red.

compared to local degradations.

Positive impact on low-level temperature bias at around 12 hour forecast range can be detected in both verifications (against ECMWF analysis and TEMP, figures 8 and 9). This partly corresponds and might be induced by a smaller fit to observations in the minimization step. The 850 hPa temperature bias is negative at the time of analysis and positive after 12-hour integration (figure 10). A larger negative analysis bias causes smaller positive bias after 12h.

The average RMSE impact is nearly neutral, but it can be noticed that the largest amplitude of impact is positive and observed for 48h temperature at 700 hPa. The corresponding time evolution of scores (bottom panel of figure 11) indicates that this positive impact is relatively robust.

A positive impact on low-level wind fields can be seen for TEMP verification over France. In higher levels, there are improvements and degradations, depending on the level and forecast range (more positive around 24, more negative around 36 hour range). But the temporal evolution of the scores (figure 12) indicates some robust reduction of RMSE at the forecast ranges between 36 and 48 hours.

Some nice significant improvement can be found for precipitation forecasts. In the verification against SYNOP observations, RMS error is reduced for almost all (except +36h) forecast ranges (figure 13). This can be seen over the large FRANX01 domain (bottom panel of Figure 13) and also over France domain (top panel of Figure 13). This positive impact on precipitation is likely to be connected with the positive impact on humidity (figures 11 and 9 - panel RMSE over France)

3.2. Case study (September 25-29 2007)

The daily evolutions of the verification scores show a high daily variation, but the experiment and reference values are often very close to each other. From time to time, the error evolutions differ a bit more. A larger sensitivity can be identified in the period between 25^{th} - 29^{th}

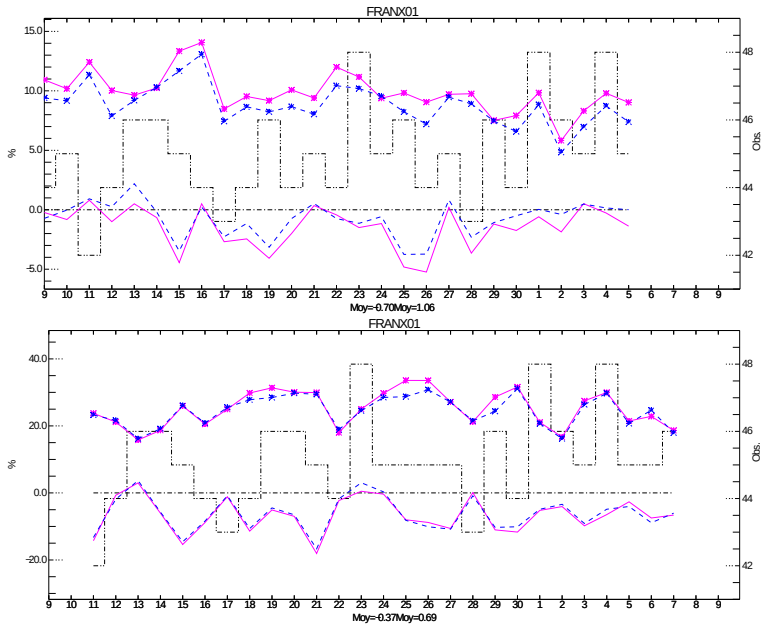

Figure 11: Daily evolution forecast RMSE and bias for specific humidity: 850 hPa analysis (top) and 700 hPa +48h forecast (bottom). All scores against TEMP observations.

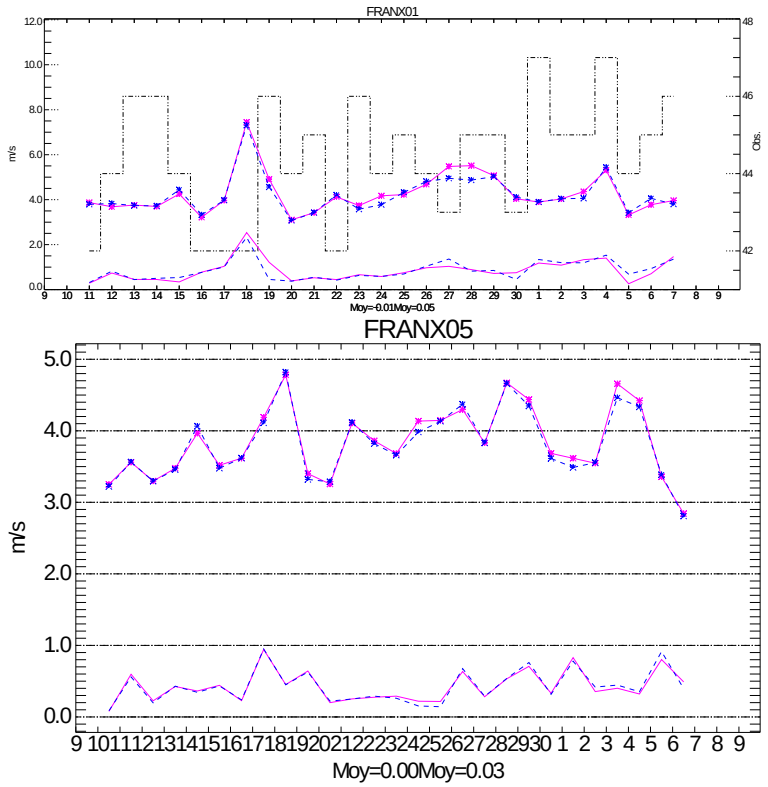

Figure 12: Daily evolution of forecast RMSE and bias for wind: 850 hPa +48h wind against TEMP (top) and 700 hPa +36h wind speed against ECMWF analysis (bottom).

September 2007. There was an outbreak of cold polar air over central Europe. It developed

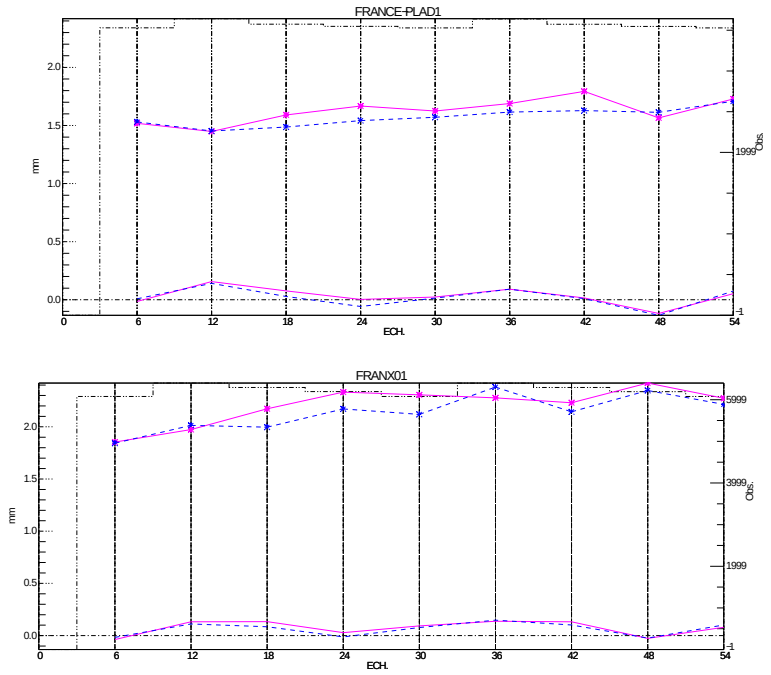

Figure 13: Daily evolution of forecast RMSE and bias for precipitation against SYNOP observations.

on 27^{th} and stayed for the few next days, slowly moving eastwards and weakening. Figure 14 presents the synoptic development and ensemble background errors for the first three days of the event at 00 UTC. We can identify two different processes in the 24-hour sequence. Firstly, the largest values of background errors over the domain can be found close to the sharpest geopotential gradients and also over the weak low in the Mediterranean on the first day. The largest values travel to the southeast with the developing wave. These are the areas where an increased weight of observations in the analysis would be appropriate. Secondly, the amplitude of the highest σ_b values is decreasing with time. This reflects the data density over sensitive areas. It is quite low over the Atlantic ocean near Ireland (first day) and gets higher when the developing passes over Europe. Together with 48-hour forecasts, the presented analysis dates cover the majority of the event. The question is if the difference in specifying σ_b's can significantly change the quality of the forecast. Experimental forecasts were compared to operational ones. To estimate the precision of the forecasts, they were verified against the subsequent analyses from their own assimilation cycles (preformed further in time). The magnitudes of differences can actually be quite high. The experimental and operational errors are quite similar most of the time. The highest errors can be found especially in the areas in front of the developing wave, where also high wind speeds and pressure gradients are present. In our case, this is mostly over central Mediterranean and Italy and Adriatic sea, at the south-east side of the cold pool. Figures 15 and 16 present the most interesting forecast quality differences for the observed period.

Significantly large improvements for wind can be illustrated for the second day for 24h and 48h forecast ranges (figure 15). This is likely to be a consequence of using flow-dependent vorticity errors. Some improvements can be found for temperature forecasts (figure 16) also. This case study suggests that forecast impacts can be relatively large and spatially localized,

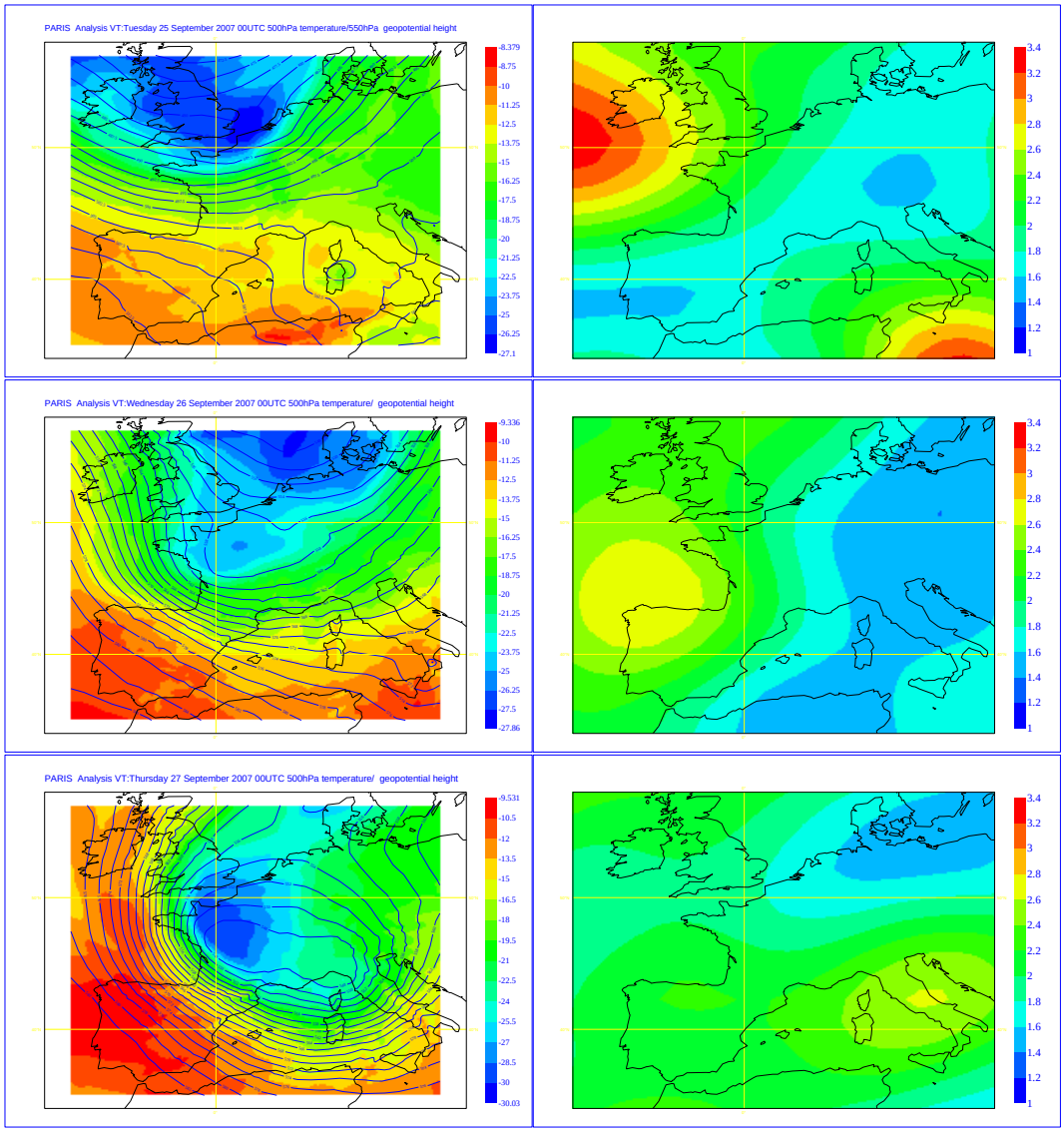

Figure 14: The meteorological situation in the period of 25^{th} - 27^{th} September 2007. Left: 500 hPa temperature (colors) and geopotential (isolines) analysis at 00 UTC, right: corresponding background errors at level 40 (approximately 500 hPa).

and thus it supports also the use of case studies and visual examination of forecast minus analysis fields, to document the impact of such changes in the assimilation system.

4. Conclusions and outlook

The grid point σ_b's of relative vorticity were successfully adapted for using in Aladin. At the same time, the specific humidity background errors were allowed to be flow dependent, using an empirical formula to compute them from background fields. For other variables, the normalization using mean spectral errors was applied. Different diagnostic and performance checks show generally a good performance of minimization using such background error

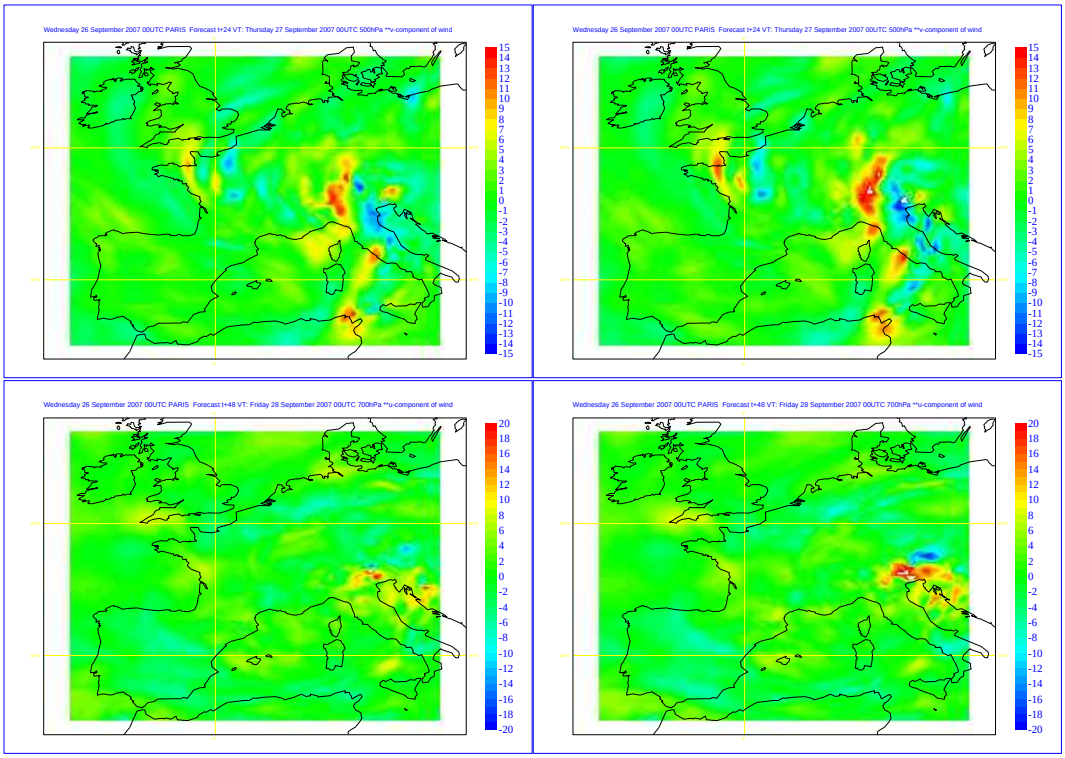

Figure 15: September 26^{th} 2007 0 UTC wind (m/s) forecast errors (left: EXP, right: OPER). 24h forecast of 500 hPa v wind component (top) and 48h forecast of 700 hPa u wind component forecast (bottom).

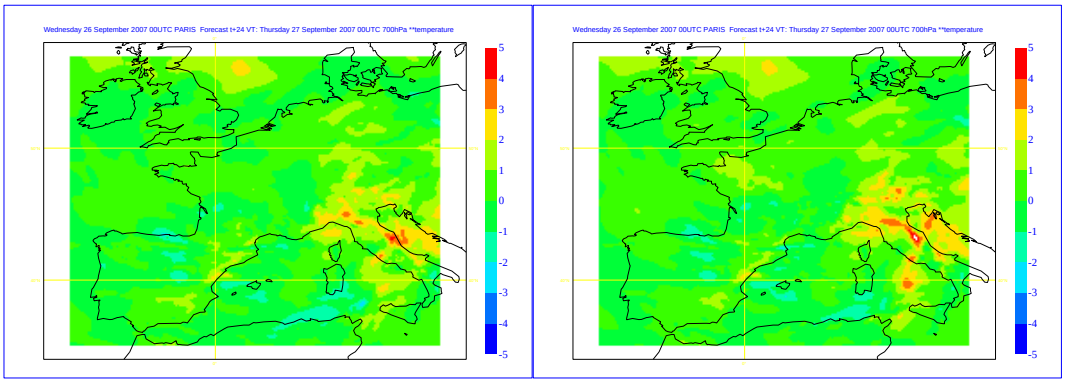

Figure 16: Errors of 24-hour temperature (K) forecasts, started on September 26^{th} 2007 0 UTC (left: EXP, right: OPER).

specification. The climatological errors might soon be used in operations, eventhough this does not not improve forecasts significantly. At least the background error specification is more realistic. Further improvements could be gained by calculating seasonal background errors, or more directly "errors of the day".

Experiments with background "errors of the day" are also considered being successful. Impact on forecast quality is generally slightly positive globally (some high error peaks are reduced etc.). A promising result was obtained for precipitation, showing a considerable improvement in verification against SYNOP. After the Arpege ensembles will be run in

operations, there is a possibility to compute and use also the daily grid point background errors in Aladin too.

The further work contains the application of ensemble background errors also to other variables. It will be soon tested for specific humidity, instead of specification by the empirical formula. For other variables it is not fully straightforward, because we have to specify the errors only for their unbalanced part (balanced part of increments, computed from total vorticity increments, are subtracted before). After solving this problem, the role of average spectral errors will be only to scale ensemble errors according to Aladin geometry.

An interesting future solution would be also to run Aladin ensemble forecasts and use them to estimate the background errors. The additional background error scaling would not be needed anymore in this case.

References

Belo Pereira, M. and L. Berre 2006: The use of an ensemble approach to study the background error covariance in a global NWP model. *Mon.Wea.Rev.*, **134**, 2466-2489.]

Berre, L., 2000 : Estimation of synoptic and mesoscale forecast error covariances in a Limited Area Model. *Mon. Wea. Rev.*, **128**, 644667.

Berre, L., Pannekoucke, O., Desroziers, G., Stefanescu, S. E., Chapnic, B. and Raynaud, L., 2007. A variational assimilation ensemble and the spatial filtering of its error covariances: increase of sample size by local spatial averaging. *Proceedings of the ECMWF workshop on Flow-dependent aspects of Data Assimilation.* ECMWF, Reading, UK, 2007, 151-168.

Rabier, F., A. McNally, E. Andersson, P. Courtier, P. Undén, J. Eyre, A. Hollingsworth and F. Bouttier, 1998: The ECMWF implementation of three dimensional variational assimilation (3D-Var). Part 2 : Struture functions. *Q. J. R. Meteorol. Soc.*, **124**, 1809-1829.

A. Experiment list

For all the presented experiments, *OLIVE swapp* environment was used. They can be found under user *mrpa*663/*SBDAY*. The names and brief description of the main experiments is given in table 1. The Aladin cycles for the experiments were chosen in a way that they match the operational (or the other) reference. For all experiments, all available observations were used (Aladin France 3DVAR operational setup). The *ClearCase* branch for the code modi-

subdir.	name	description
test runs	7393	test for using grid point σ_b's
single obs	73A9	single radiosonde obs. experiment
	73CA	single obs. for WINTER period
	73CB	single obs. for SUMMER period
SBDAY	73C4	daily σ_b impact run for Sep/Oct 2007
impact runs	B0AR	climatological grid point σ_b's, WINTER impact run
	739U	climatological grid point σ_b's, SUMMER impact run

Table 1: Overview of the main used experiments.

fications to enable grid point background errors is *arp_mrpa*683_*CY*33_*sbgdp_nlhum*. In this contribution, the modifications are merged with those to enable nonlinear humidity variable change. On *tori* supercomputer, the corresponding packs are *mrpa*683/*pack*/*COMMON* (al32t1) and *mrpa*683/*pack*/*COMMON_CY*33 (al33t0).

B. Grid point σ_b technical documentation

B.1. Preparation of grid point σ_b's for Aladin

Gridpoint standard deviations of background error, simulated by an ensemble of analyses, are stored in grib files named errgrib. Until now, only vorticity standard deviations were used (stored in the file called Errgribvor). Grid point background error specification is chosen by a switch LSPFCE=.F. (whereas LSPFCE=.T. corresponds to error normalization in spectral space, using horizontally constant background errors) in namelist YOMJG. In this case, at least vorticity or wind error standard deviations have to be provided in the errgrib files. Grid point background errors are initialized in routine SUINFCE, called from setup routine SU0YOMB. Errgrib file is examined and read via the input/output subroutines IO_INQUIRE and IO_GET. Depending on the values of switch LSBLATLONG from namelist NAMJG, the lat/lon or gaussian grid is expected. The default value is false (errors specified in gaussian grid). Error standard deviations are then horizontally (SUHIFCE) and vertically (SUVIFCE) interpolated from input error grid to model grid (e.g. Aladin geometry). Background field are also needed for computation of humidity background errors. They are provided from the trajectory files (GET_TRAJ_GRID) or from spectral arrays, using inverse Fourier transform (INV_TRANS). Background error standard deviations for the variables which are not present in errgrib files are determined from global spectral averages (as specified in *stabal* files). The only exception is for specific humidity errors. They are determined using a simple

relationship with relative humidity errors, which are computed by an empirical formula (based on radiosonde data departures) using background values of temperature and relative humidity itself (Rabier et al., 1998; routine SUSHFCE). Global mean average profiles of

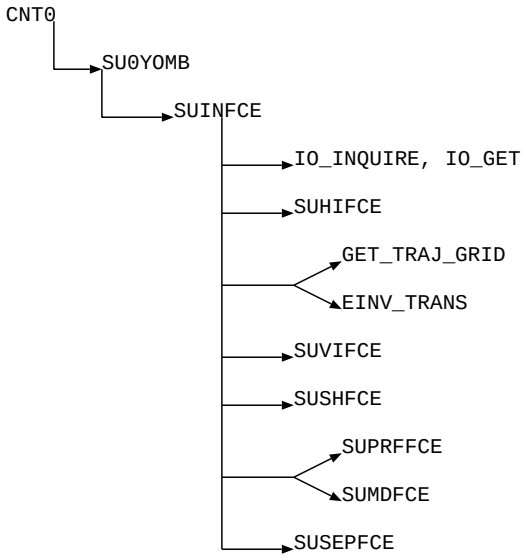

Figure 17: Calling tree for SUINFCE.

background errors are then calculated in SUPRFFCE. The averaging is weighted using grid point area. (Optionally (this is not the default approach), it is possible to separate horizontal and vertical variations of background errors (SUMDFCE, if L3DBGERR = .F.). This is done by computing a pressure weighted vertical integral of background errors, multiplied by spectral background errors and normalized by a gridbox area. The global area-weighted average of this pattern is 1. Actual background errors for a given geographical location can then be recalculated by multiplication of pattern by average spectral error.)

The next step (SUSEPFCE) is to multiply background error standard deviations by the ratio between global spectral averages and globally averaged profiles of grid point errors. This is done to ensure that mean background errors (e.g. if used for a single day) correspond to prescribed global averages (specified in *stabal* files). Optionally, the spectral errors are multiplied by horizontal pattern, computed in SUMDFCE. The last step is to apply a map factor (depending on geographical position) to vorticity and divergence standard deviations. Background errors of vorticity and unbalanced parts of divergence, temperature and mean sea level pressure are now determined and copied in the background error buffer, which is then used for background error normalization in the minimization process.

B.2. Multiplication by σ_b's inside minimization

Prescribed background errors are used inside minimization, more exactly in the variable change from control to model space (routine CHAVARIN). After accounting for correlations and before solving balance relationships, the control variable increments are multiplied by grid point standard deviations of background error. This is done inside routine CVARGPTL, in the subroutine EJGNRGGI in the case of Aladin. (At this stage, an option

LEVARGP=.TRUE. (which is not the default value) is also provided for zeroing the increments in I+E zones in order to prevent the bi-periodic structures to affect the opposite side of limited area domain. The background errors are multiplied by a weighting function which is falling from one to zero throughout the I zone, becoming equal zero in the E zone.)